Proceedings of IMECE2004
2004 ASME International Mechanical Engineering Congress and RD&D Expo
November 13-19, 2004, Anaheim, California USA

IMECE2004-61289

OBSERVER BACKSTEPPING NEURO-FUZZY CONTROL DESIGN FOR A TYPE OF NONLINEAR SYSTEM

Withit Chatlatanagulchai
Motion and Vibration Control Laboratory,
School of Mechanical Engineering,
Purdue University. (e-mail: chatlata@purdue.edu).

Peter H. Meckl
Motion and Vibration Control Laboratory,
School of Mechanical Engineering,
Purdue University. (e-mail: meckl@purdue.edu;
phone: 765-494-0539; fax: 765-494-5686).

ABSTRACT

This paper presents a control system design for a type of time-varying nonlinear system. The control system comprises neuro-fuzzy system identifier, Luenberger observer, backstepping controller and variable structure controller. We use adaptive neuro-fuzzy inference system to identify the plant in real time without the need of underlying mathematical model. However, some knowledge about the plant structure and upper bounds is required. With the use of observer, the control system can be designed from plant output and input alone while plant states are assumed unmeasurable. Controller is designed based on backstepping scheme and uncertainties from the plant identification and state estimation processes are handled by variable structure controller. Under some important assumptions, the control system is proved to be able to track a smooth desired trajectory with uniformly ultimately bounded tracking error. A simulation based on one-link flexible-joint robot manipulator is provided.

Keywords: Backstepping, Variable structure control, Neuro-fuzzy, Luenberger observer, Nonlinear systems.

1. INTRODUCTION

Recently, researchers have used intelligent systems such as neural networks and fuzzy logic to identify the plant model without having to refer to its physical laws. The methods are powerful due to their ability to approximate continuous nonlinear functions to any arbitrary accuracy, as shown in [1]-[3]. The unknown parameters need not appear linearly and disturbances and uncertainties are handled naturally. Intelligent system continuously adapts to the actual plant during the identification process. One of the earliest works appeared in [4] where multilayer neural networks were used to identify the whole plant off-line and control design was based on inverse dynamics and PD control. Reference [5] includes many examples of this type of control scheme and more sophisticated intelligent systems were used in [6], [7].

The control system presented in this paper is depicted in Fig. 1. The applicable plant has similar structure to the strict feedback form. The difference is that nonlinear functions in our plant can be functions of all states. The plant is assumed to depend explicitly on time. We use a type of neuro-fuzzy system called adaptive neuro-fuzzy inference system (ANFIS) to identify plant functions in real time. Neuro-fuzzy system uses neural network structure to provide fuzzy system with automatic tuning abilities. Both membership functions and fuzzy rules can be tuned based on specified performance objectives. ANFIS was introduced in [8] and was proved to be a universal approximator in [9]. We use a Luenberger-type observer similar to that in [10].

The controller is based on backstepping design scheme. One can view backstepping as feedback linearization in subsystem level where only one state equation is considered at a time. Fictitious input of each step is constructed such that it cancels nonlinearities and reduces the error between each state and its desired value resulting in overall stabilized closed-loop system. Backstepping design scheme for systems in strict-feedback form is discussed extensively in [11] where additional disturbances are usually handled by nonlinear damping terms. A disadvantage in using nonlinear damping terms to provide robustness to the control system is that the disturbances or uncertainties must be multiplied by known functions which may not always be the case.

In this paper we use variable structure control (VSC) similar to that in [12] and [13]. The VSC requires uncertainties to be bounded however the bounds need not be known. In theory, we are able to obtain zero tracking error with

discontinuous VSC and uniformly ultimately bounded error with smooth VSC. The controller makes use of identified plant functions. Therefore, it may be called indirect approach to be consistent with the adaptive control community.

This paper is organized as follows. In Section 2, we present applicable system description and identifier design. Observer and controller designs are presented in Section 3 and Section 4 respectively. A simulation of one-link flexible-joint robot manipulator is given in Section 5, which is followed by our conclusion section. Appendices are details of the stability proofs.

2. SYSTEM DESCRIPTION AND IDENTIFIER DESIGN

In this paper, we consider applicable plants in the form:

$$\begin{aligned} \dot{x}_i &= f_i(\bar{x}_m,t) + g_i(\bar{x}_m,t)x_{i+1}, \quad 1 \le i \le m-1, \\ \dot{x}_m &= f_m(\bar{x}_m,t) + g_m(\bar{x}_m,t)u, \\ y &= x_1, \end{aligned} \tag{1}$$

where $x_i \in \mathbb{R}, u \in \mathbb{R}, y \in \mathbb{R}$, $\bar{x}_i = \{x_1,\ldots,x_i\}$, $f_i(\bullet), g_i(\bullet)$ are unknown smooth functions. Only output y is measurable.

Since $f_i(\bullet), g_i(\bullet)$ are smooth, each of them can be approximated by neuro-fuzzy system in Fig. 2 to any arbitrary accuracy. Suppose, there are i inputs and j rules. Layer 1 performs fuzzification by assigning membership function to each input. It is clear that if f_i is a function of $x_1,\ldots,x_m$, then $x_1,\ldots,x_m$ are inputs to the neuro-fuzzy system. There are many types of membership functions, we use bell-shaped functions which can be put as follows:

$$\mu_{i,j}(x_i) = 1/\left(1+\left(\left(x_i - c_{i,j}\right)/a_{i,j}\right)^{2b_{i,j}}\right),$$

where $a_{i,j}, b_{i,j}, c_{i,j}$ are premise parameters. Layer 2 output represents firing strength of each fuzzy rule by performing "and" operation:

$$W_k = \prod_{l=1}^{i} \mu_{l,j}, \ k = 1,\ldots,j.$$

Layer 3 normalizes firing strengths with output:

$$\bar{W}_k = W_k / \left(\sum_{l=1}^{j} W_l\right), \ k = 1,\ldots,j.$$

Layer 4 represents output of each fuzzy rule:

$$\bar{W}_k \left(v_{k,i+1} + \sum_{l=1}^{i} v_{k,l}x_l\right), \ k = 1,\ldots,j,$$

where $v_k = \left[v_{k,1}, v_{k,2},\ldots, v_{k,i+1}\right] \in \mathbb{R}^{i+1}$ is a vector contain consequent parameters. The output of Layer 5 is given by:

$$\hat{f} = \sum_{k=1}^{j} \bar{W}_k \left(v_{k,i+1} + \sum_{l=1}^{i} v_{k,l}x_l\right). \tag{2}$$

$\hat{f}$ is the estimation of f. Various learning schemes can be seen in [9]. In this paper, for convenience, we fix premise parameters and adjust only consequent parameters online using recursive least square (RLS) method.

Consider the first equation of (1), suppose first that all states are measurable, we have

$$\dot{x}_1 = \hat{f}_1(\bar{x}_m,t) + \hat{g}_1(\bar{x}_m,t)x_2, \tag{3}$$

where $\hat{f}_1, \hat{g}_1$ are estimated functions of f_1, g_1 respectively. Each of $\hat{f}_1$ and $\hat{g}_1$ is represented by one neuro-fuzzy system. For convenience, we use J fuzzy rules for both $\hat{f}_1, \hat{g}_1$. From (2) , we have

$$\hat{f}_1 = \sum_{k=1}^{J} \bar{W}_{k,f_1} \left(v_{k,1,f_1}x_1 + v_{k,2,f_1}x_2 + \ldots + v_{k,m,f_1}x_m + v_{k,m+1,f_1}\right),$$

$$\hat{g}_1 = \sum_{k=1}^{J} \bar{W}_{k,g_1} \left(v_{k,1,g_1}x_1 + v_{k,2,g_1}x_2 + \ldots + v_{k,m,g_1}x_m + v_{k,m+1,g_1}\right).$$

Equation (3) can be put in the following regression form

$$Y = \Phi\Theta,$$

where $Y = \left[\dot{x}_1\right]$,

$$\begin{aligned} \Phi = \Big[& \bar{W}_{1,f_1}x_1,\ldots,\bar{W}_{1,f_1}x_m,\bar{W}_{1,f_1},\ldots,\bar{W}_{J,f_1}x_1,\ldots,\bar{W}_{J,f_1}x_m,\bar{W}_{J,f_1},\bar{W}_{1,g_1}x_1x_2 \\ & ,\ldots,\bar{W}_{1,g_1}x_mx_2,\bar{W}_{1,g_1}x_2,\ldots,\bar{W}_{J,g_1}x_1x_2,\ldots,\bar{W}_{J,g_1}x_mx_2,\bar{W}_{J,g_1}x_2 \ \Big], \\ \Theta = \Big[& v_{1,1,f_1},\ldots,v_{1,m,f_1},v_{1,m+1,f_1},\ldots,v_{J,1,f_1},\ldots,v_{J,m,f_1},v_{J,m+1,f_1},v_{1,1,g_1} \\ & ,\ldots,v_{1,m,g_1},v_{1,m+1,g_1},\ldots,v_{J,1,g_1},\ldots,v_{J,m,g_1},v_{J,m+1,g_1}\Big]^T. \end{aligned}$$

Vector Y and matrix Φ are known. Vector Θ can be found using recursive least square algorithm. Details of RLS algorithm as well as some practical issues during implementation can be found in [14].

Identification of the remaining state equations of (1) can be done in similar manner. Since states are not measurable, all actual states x_i and their derivatives $\dot{x}_i$ in the neuro-fuzzy system (2) will be replaced by their estimates $\hat{x}_i$ and $\dot{\hat{x}}_i$ respectively.

The identified system equations can be written as follows:

$$\begin{aligned} \dot{\xi}_i &= \hat{f}_i\left(\bar{\xi}_m\right) + \hat{g}_i\left(\bar{\xi}_m\right)\xi_{i+1}, \quad 1 \le i \le m-1, \\ \dot{\xi}_m &= \hat{f}_m\left(\bar{\xi}_m\right) + \hat{g}_m\left(\bar{\xi}_m\right)u, \\ \zeta &= \xi_1, \end{aligned} \tag{4}$$

where $\hat{f}_i, \hat{g}_i$ are estimates of f_i, g_i, ξ_i and ζ are states and output of the identified system, respectively.

3. OBSERVER DESIGN

Consider the actual plant (1), we obtain the sequence of output derivatives as follows:

$$\begin{aligned} y &= x_1, \\ \dot{y} &= f_1(\bar{x}_m,t) + g_1(\bar{x}_m,t)x_2 = \varphi_1\left(\bar{x}_m,t\right), \\ y^{(2)} &= \frac{\partial\varphi_1}{\partial t} + \sum_{i=1}^{m-1}\left\{\frac{\partial\varphi_1}{\partial x_i}\left[f_i(\bar{x}_m,t) + g_i(\bar{x}_m,t)x_{i+1}\right]\right\} \end{aligned}$$

$$
\begin{aligned}
&+\frac{\partial \varphi_1}{\partial x_m}\left[f_m(\bar{x}_m,t)+g_m(\bar{x}_m,t)u\right]\\
&=\varphi_2\left(\bar{x}_m,u,t\right),\\
&\vdots\\
&y^{(m-1)}=\varphi_{m-1}(\bar{x}_m,u,\dot{u},u^{(2)},\ldots,u^{(m-3)},t).
\end{aligned}
\tag{5}
$$

We then have the mapping relating the first $m-1$ derivatives of the output y to the states of the system and the input derivatives as follows:

$$
\begin{aligned}
y_e&=\left[\begin{array}{cccc} y & \dot{y} & \ldots & y^{(m-1)}\end{array}\right]^T=H(\bar{x}_m,u,\dot{u},u^{(2)},\ldots,u^{(m-3)},t)\\
&=\left[\begin{array}{cccc} x_1 & \varphi_1(\bar{x}_m,t) & \ldots & \varphi_{m-1}(\bar{x}_m,u,\dot{u},u^{(2)},\ldots,u^{(m-3)},t)\end{array}\right]^T.
\end{aligned}
\tag{6}
$$

Similarly, consider the identified plant (4), we obtain equations similar to (5) and (6) for the identified system as follows:

$$
\begin{aligned}
&\zeta=\xi_1,\\
&\dot{\zeta}=\hat{f}_1(\bar{\xi}_m)+\hat{g}_1(\bar{\xi}_m)\xi_2=\psi_1\left(\bar{\xi}_m\right),\\
&\vdots\\
&\zeta^{(m-1)}=\psi_{m-1}(\bar{\xi}_m,u,\dot{u},u^{(2)},\ldots,u^{(m-3)}),
\end{aligned}
\tag{7}
$$

$$
\begin{aligned}
\zeta_e&=\left[\begin{array}{cccc} \zeta & \dot{\zeta} & \ldots & \zeta^{(m-1)}\end{array}\right]^T=\hat{H}(\bar{\xi}_m,u,\dot{u},u^{(2)},\ldots,u^{(m-3)})\\
&=\left[\begin{array}{cccc} \xi_1 & \psi_1(\bar{\xi}_m) & \ldots & \psi_{m-1}(\bar{\xi}_m,u,\dot{u},u^{(2)},\ldots,u^{(m-3)})\end{array}\right]^T.
\end{aligned}
\tag{8}
$$

Replacing identified state ξ_i with the estimated state $\hat{x}_i$, we have

$$
\begin{aligned}
\hat{\zeta}_e&=\left[\begin{array}{cccc} \hat{\zeta}_{e_1} & \hat{\zeta}_{e_2} & \ldots & \hat{\zeta}_{e_m}\end{array}\right]^T\\
&=\hat{H}(\bar{\hat{x}}_m,u,\dot{u},u^{(2)},\ldots,u^{(m-3)})\\
&=\left[\begin{array}{cccc} \hat{x}_1 & \psi_1(\bar{\hat{x}}_m) & \ldots & \psi_{m-1}(\bar{\hat{x}}_m,u,\dot{u},u^{(2)},\ldots,u^{(m-3)})\end{array}\right]^T.
\end{aligned}
\tag{9}
$$

Assumption 1: System (1) and identified system (4) are uniformly completely observable, i.e., the mapping $H(\bar{x}_m,u,\dot{u},u^{(2)},\ldots,u^{(m-3)},t)$ and $\hat{H}(\bar{\xi}_m,u,\dot{u},u^{(2)},\ldots,u^{(m-3)})$ are invertible with respect to $\bar{x}_m$ and $\bar{\xi}_m$ and their inverses, $H^{-1}(y_e)$ and $\hat{H}^{-1}\left(\zeta_e\right)$, are smooth. Moreover, if $\left\|y_e-\zeta_e\right\|\le\varepsilon_1$ for some $\varepsilon_1>0$, then $\left\|H^{-1}\left(y_e\right)-\hat{H}^{-1}\left(\zeta_e\right)\right\|\le\varepsilon_2$ for some finite $\varepsilon_2>0$.

From (5), we have

$$
\begin{aligned}
y^{(m)}&=\dot{\varphi}_{m-1}(\bar{x}_m,u,\dot{u},u^{(2)},\ldots,u^{(m-3)},t)\\
&=\sum_{k=1}^{m-2}\left\{\frac{\partial\varphi_{m-1}}{\partial u^{(k-1)}}u^{(k)}\right\}+\sum_{l=1}^{m-1}\left\{\frac{\partial\varphi_{m-1}}{\partial x_l}\left[f_l(\bar{x}_m,t)+g_l(\bar{x}_m,t)x_{l+1}\right]\right\}\\
&+\frac{\partial\varphi_{m-1}}{\partial x_m}\left[f_m(\bar{x}_m,t)+g_m(\bar{x}_m,t)u\right]+\frac{\partial\varphi_{m-1}}{\partial t}\\
&=\alpha\left(\bar{x}_m,t\right)+\beta_1\left(\bar{x}_m,t\right)u+\ldots+\beta_{m-1}\left(\bar{x}_m,t\right)u^{(m-2)}.
\end{aligned}
\tag{10}
$$

Then, from (6), we have

$$
\dot{y}_e=Ay_e+B\left[\alpha\left(y_e\right)+\beta_1\left(y_e\right)u+\ldots+\beta_{m-1}\left(y_e\right)u^{(m-2)}\right],
\tag{11}
$$

where

$$
A=\begin{bmatrix}0&&\\ \vdots & I&\\ 0&\cdots&0\end{bmatrix},\quad B=\begin{bmatrix}0&\ldots&0&1\end{bmatrix}^T.
$$

We obtain similar equations to (10) and (11) for the identified system as follows:

$$
\begin{aligned}
\zeta^{(m)}&=\dot{\psi}_{m-1}(\bar{\xi}_m,u,\dot{u},u^{(2)},\ldots,u^{(m-3)})\\
&=\hat{\alpha}\left(\bar{\xi}_m\right)+\hat{\beta}_1\left(\bar{\xi}_m\right)u+\ldots+\hat{\beta}_{m-1}\left(\bar{\xi}_m\right)u^{(m-2)},
\end{aligned}
$$

$$
\dot{\zeta}_e=A\zeta_e+B\left[\hat{\alpha}\left(\zeta_e\right)+\hat{\beta}_1\left(\zeta_e\right)u+\ldots+\hat{\beta}_{m-1}\left(\zeta_e\right)u^{(m-2)}\right].
$$

Assumption 2: The differences between actual functions f_i, g_i in (1) and their estimates $\hat{f}_i$, $\hat{g}_i$ in (4) are bounded.

Assumption 3: Control input u is bounded and continuous differentiable to the order of $m-2$.

With Assumption 1, 2 and 3 in place, we are now ready to state the following proposition.

Proposition 1: Using nonlinear observer

$$
\begin{aligned}
&\begin{bmatrix}\dot{\hat{x}}_1\\ \dot{\hat{x}}_2\\ \vdots\\ \dot{\hat{x}}_m\end{bmatrix}=\begin{bmatrix}\hat{f}_1(\bar{\hat{x}}_m)+\hat{g}_1(\bar{\hat{x}}_m)\hat{x}_2\\ \hat{f}_2(\bar{\hat{x}}_m)+\hat{g}_2(\bar{\hat{x}}_m)\hat{x}_3\\ \vdots\\ \hat{f}_m(\bar{\hat{x}}_m)+\hat{g}_m(\bar{\hat{x}}_m)u\end{bmatrix}+\left[\frac{\partial\hat{H}(\bar{\hat{x}}_m)}{\partial\bar{\hat{x}}_m}\right]^{-1}\varepsilon^{-1}L\left[y-\hat{x}_1\right],\\
&\hat{\zeta}=\hat{x}_1,
\end{aligned}
\tag{12}
$$

where $\varepsilon=diag\left[\eta,\eta^2,\ldots,\eta^m\right]$, $0<\eta\le1$ and $\left[\partial\hat{H}(\bar{\hat{x}}_m)/\partial\bar{\hat{x}}_m\right]$ is the Jacobian of $\hat{H}$, η is a design parameter and $L=[l_1,l_2,\ldots,l_m]^T$ is such that $s^m+l_1s^{m-1}+\ldots+l_m$ is a Hurwitz polynomial. Then, the estimation error, $\tilde{\zeta}_e=\hat{\zeta}_e-y_e$, is globally uniformly ultimately bounded.

Proof: See Appendix A.

4. CONTROLLER DESIGN

Our objective is to make the output $y=x_1$ track reference trajectory x_{1d} as closely as possible, while all the signals in the closed-loop system are bounded. In addition to the assumptions in the previous sections, we also need the following.

Assumption 4: There exist known constants $g_{iU}>0$ such that $\left\|g_i(\cdot)\right\|\le g_{iU}\quad\forall i=1,\ldots,m$.

We proceed by letting $z_1=\hat{x}_1-x_{1d}$ be the error between the estimated state $\hat{x}_1$ and the desired output. We then have the derivative of the error as follows:

$$
\dot{z}_1=\dot{\hat{x}}_1-\dot{x}_{1d}=\dot{x}_1+\dot{\hat{x}}_1-\dot{x}_{1d}=f_1+g_1x_2+\dot{\hat{x}}_1-\dot{x}_{1d}.
$$

Let x_{2d} be the virtual control input of this step and introduce the error variable $z_2=\hat{x}_2-x_{2d}$. We can see that if we can find a way to make z_2 small, we will have $\hat{x}_2\approx x_{2d}$ and hence $x_2\approx x_{2d}$. This fact will be shown in the proof to follow. For

now, let us assume that $x_2 \approx x_{2d}$ and therefore, the virtual control input x_{2d} has the form

$$x_{2d} = -\hat{g}_1^{-1}\left(c_1 z_1 + \hat{f}_1 - \dot{x}_{1d} + u_{2dvsc}\right).$$

Intuitively, this controller can be explained as follows. The $\hat{g}_1^{-1}$ and $\hat{f}_1$ terms are used for linearizing the subsystem by canceling the nonlinear terms. The $c_1 z_1$ term is used as proportional gain to drive the error z_1 to a small value. $\dot{x}_{1d}$ is to cancel with the $\dot{x}_{1d}$ in the error equation. The variable structure control input u_{2dvsc} provides robustness against uncertainties arising from state estimation error and plant identification error.

From Assumption 2, we have $\left|f_1 - \hat{f}_1\right| \le \varepsilon_{f_1}, \left|g_1 - \hat{g}_1\right| \le \varepsilon_{g_1}$, where $\varepsilon_{f_1}, \varepsilon_{g_1}$ are bounded positive constants. From Assumption 4, we have $\left|g_1\right| \le g_{1U}$. From Proposition 1, we know that the state estimation error $\tilde{\zeta}_e = \hat{\zeta}_e - y_e$ is globally uniformly ultimately bounded and therefore together with Assumption 1 we have that $\tilde{x}_2 = \hat{x}_2 - x_2$ is bounded, that is, $\left|\tilde{x}_2\right| \le \varepsilon_{x_2}$, where ε_{x_2} is bounded positive constant. Since $\hat{x}_1$ and x_1 are smooth (this fact can be seen from looking at each component in the actual state equations (1), the observer equations (12) and the fact that the actual control input u is smooth), we have $\left|\dot{\tilde{x}}_1\right| \le \varepsilon_{\dot{x}_1}$ where $\varepsilon_{\dot{x}_1}$ is bounded positive constant. Put everything together, we have the following inequality:

$$\left|f_1 - \hat{f}_1\right| + \left|\left(g_1 - \hat{g}_1\right) x_{2d}\right| + \left|g_1 \tilde{x}_2\right| + \left|\dot{\tilde{x}}_1\right| \le K_1^{*T} \varphi_1,$$

where

$$K_1^* = \left[\varepsilon_{f_1}, \varepsilon_{g_1}, \varepsilon_{x_2}, \varepsilon_{\dot{x}_1}\right]^T,$$

$$\varphi_1 = \left[1, \left\|x_{2d}\right\|, g_{1U}, 1\right]^T.$$

We let the smooth variable structure control term be in the form

$$u_{2dvsc} = \hat{K}_1^T \overline{\varphi}_1, \tag{13}$$

where

$$\overline{\varphi}_1 = \left[\frac{2}{\pi}\arctan\left(\frac{z_1}{\mu_1}\right), \left\|x_{2d}\right\|\frac{2}{\pi}\arctan\left(\frac{z_1}{\mu_1\left\|x_{2d}\right\|}\right),\right.$$

$$\left. g_{1U}\frac{2}{\pi}\arctan\left(\frac{z_1}{\mu_1} g_{1U}\right), \frac{2}{\pi}\arctan\left(\frac{z_1}{\mu_1}\right)\right]^T,$$

μ_1 is a small positive number. $\hat{K}_1$ approximates K_1^* with following update law:

$$\dot{\hat{K}}_1 = \dot{\hat{K}}_1 = \Gamma_{k1}[\overline{\varphi}_1 z_1 - \sigma_{k1}\hat{K}_1], \tag{14}$$

where $\Gamma_{k1} > 0, \sigma_{k1} > 0$ are design parameters. The σ_{k1} term in the update law is used to prevent $\hat{K}_1$ from growing unboundedly by maintaining its value around the initial value.

Let us now proceed by the same manner as before. By letting $z_i = \hat{x}_i - x_{id}$ where $2 \le i \le m-1$, we have the derivative of the error as

$$\dot{z}_i = \dot{\hat{x}}_i - \dot{x}_{id} = \dot{x}_i + \dot{\tilde{x}}_i - \dot{x}_{id} = f_i + g_i x_{i+1} + \dot{\tilde{x}}_i - \dot{x}_{id}.$$

The virtual control input $x_{(i+1)d}$ has the form

$$x_{(i+1)d} = -\hat{g}_i^{-1}\left(g_{(i-1)U} z_{i-1} + c_i z_i + \hat{f}_i - \dot{x}_{id} + u_{(i+1)dvsc}\right),$$

where the extra term $g_{(i-1)U} z_{i-1}$ is used to cancel the effect of a term from the previous step for the Lyapunov stability proof to follow. The variable structure control input $u_{(i+1)dvsc}$ and the update law $\hat{K}_i$ are similar to the previous step.

For the last step where $i = m$, we have the actual control input u in the similar form

$$u = -\hat{g}_m^{-1}\left(g_{(m-1)U} z_{m-1} + c_m z_m + \hat{f}_m - \dot{x}_{md} + u_{(m+1)dvsc}\right). \tag{15}$$

We are now ready to state the following proposition.

Proposition 2: Consider the closed-loop system consisting of actual plant (1), observer (12), identifier (4), controller (15) with variable structure controller (13) and update law (14). Then, for bounded initial conditions, all errors z_i and $\tilde{K}_i$ are globally uniformly ultimately bounded. Moreover, they eventually converge to a compact set

$$\Omega \triangleq \left\{z_i, \tilde{K}_i,\ i = 1, \ldots, m \middle| V_m \le \frac{\delta}{\varsigma}\right\}$$

where $\varsigma = \min_{1 \le l \le m}\{2c_l\} > 0$, $\delta = \sum_{l=1}^{m} \chi_l \ge 0$,

$$\chi_l = 0.2785\eta_l\left(\varepsilon_{f_l} + \varepsilon_{g_l} + \varepsilon_{x_{l+1}} + \varepsilon_{\dot{x}_l}\right) + \frac{\sigma_{kl}}{2}\left\|K_l^*\right\|^2.$$

Proof: See Appendix B.

5. SIMULATION RESULTS

Consider the one-link flexible-joint robot manipulator in the vertical plane as in Fig. 3. Controller design for flexible-joint manipulator based on backstepping and three-layer neural networks can be seen in [17]. The manipulator can be put in state-space representation as

$$\dot{x}_1 = x_2,$$

$$\dot{x}_2 = \frac{1}{\left(m_l a^2 + J_l + m_p b^2 + J_p\right)}[-k x_1 - \left(m_l a + m_p b\right) g \sin x_1$$

$$-\left(c_l + d\right) x_2 + \frac{k}{r} x_3 + \frac{d}{r} x_4],$$

$$\dot{x}_3 = x_4,$$

$$\dot{x}_4 = \frac{1}{\left(J_m + \frac{J_s}{r^2}\right)}\left(\frac{k}{r} x_1 + \frac{d}{r} x_2 - \frac{k}{r^2} x_3 - \left(c_m + \frac{d}{r^2}\right) x_4 + u\right),$$

$$y = x_1,$$

where $x_1 = \theta_l, x_2 = \dot{\theta}_l, x_3 = \theta_m, x_4 = \dot{\theta}_m, u = T$. Table 1 shows description of parameters as well as their values used in the simulation.

Our objective is to make the output track a signal, obtained from passing a square wave of amplitude 10, zero mean, and

20-sec period into the filter $1/(s+2)^3$, as closely as possible. We choose sampling period to be 0.01 sec.

For identifier (4), we use forgetting factor $\lambda = 0.995$, number of fuzzy rules for each input $J = 2$, $P_0 = 10^6 I$. Premise parameters of each input are fixed as follows:

$a_{1,1} = 1/3,\ a_{1,2} = 1/3,\ b_{1,1} = 1,\ b_{1,2} = 1,\ c_{1,1} = -1/3,\ c_{1,2} = 1/3,$

$a_{2,1} = 1/6,\ a_{2,2} = 1/6,\ b_{2,1} = 1,\ b_{2,2} = 1,\ c_{2,1} = -1/6,\ c_{2,2} = 1/6,$

$a_{3,1} = 10/3,\ a_{3,2} = 10/3,\ b_{3,1} = 1,\ b_{3,2} = 1,\ c_{3,1} = -10/3,$

$c_{3,2} = 10/3, a_{4,1} = 10/6,\ a_{4,2} = 10/6,\ b_{4,1} = 1,\ b_{4,2} = 1,$

$c_{4,1} = -10/6,\ c_{4,2} = 10/6.$

Θ_0 is set equal to a zero vector.

For observer (12), we have $\eta = 0.1$, $L = [10\ \ 10\ \ 20\ \ 20]^T$.

For controller (15), $\Gamma_{ki} = 1, \sigma_{ki} = 0.1, c_i = 15, g_{(i-1)U} = 1,$ $\mu_i = 0.1, \forall i = 1,\ldots,m.$

All initial values, otherwise stated, are set equal to 0.01.

First, we would like to see how the control system can adapt under model variation. We simulate the situation where payload is changed from m_p = 1 kg to m_p = 4 kg at 15 sec and back to 1 kg at 25 sec. Fig. 4 shows the tracking performance by plotting actual output $y = x_1$ versus desired trajectory $y_d = x_{1d}$. We can see that at 15 and 25 sec. where there are sudden changes in payload, the control system is able to adapt and delivers good tracking performance.

Second, we fix payload at $m_p = 1\,kg.$ and run the simulation for 100 sec. Fig. 5 shows the tracking performance by plotting the actual output y, desired output y_d, estimated state $\hat{y} = \hat{x}_1$ and identifier state $y_i = \xi_1$. We can see that the control system achieves good performance. Fig. 6 shows the membership functions of each input to the neuro-fuzzy system. Fig. 7 shows the comparison between actual plant functions f_2, g_2, f_4, g_4 and identified plant functions $\hat{f}_2, \hat{g}_2, \hat{f}_4, \hat{g}_4$. The identified functions are close to their actual values. Note that we did not identify f_1, g_1, f_3, g_3 since their values are fixed according to the structure of this state-space model. Fig. 8 shows the actual control input u and the virtual control inputs x_{2d}, x_{3d}, x_{4d}. Input u is not smooth due to the discrete-time implementation.

6. CONCLUSION

We have presented a control system, a composition of a type of neuro-fuzzy identifier, Luenberger observer and backstepping controller. Under some assumptions about the plant structure, this control system can be used when a closed-form plant model is not available. The control system is able to handle uncertainties naturally. The tracking error is proved to be globally ultimately uniformly bounded where bound can be made small by appropriately adjusting the design parameters.

APPENDIX A: PROOF OF PROPOSITION 1

All derivatives of $\hat{\xi}_{e_i}$ in (9) can be found as follows:

For $i = 1$,

$$\dot{\hat{\xi}}_{e_1} = \dot{\hat{x}}_1 = \hat{\xi}_{e_2} + I_1\left[\partial \hat{H}(\bar{\hat{x}}_m)/\partial \bar{\hat{x}}_m\right]^{-1} \varepsilon^{-1} L\left[y - \hat{x}_1\right].$$

For $i = 2$,

$$\dot{\hat{\xi}}_{e_2} = \dot{\psi}_1\left(\bar{\hat{x}}_m\right) = \hat{\xi}_{e_3} + \sum_{l=1}^{m}\left\{\frac{\partial \psi_1}{\partial \hat{x}_l}\left[I_l\left[\partial \hat{H}(\bar{\hat{x}}_m)/\partial \bar{\hat{x}}_m\right]^{-1} \varepsilon^{-1} L\left[y - \hat{x}_1\right]\right]\right\}.$$

For $3 \le i \le m-1$,

$$\dot{\hat{\xi}}_{e_i} = \dot{\psi}_{i-1}\left(\bar{\hat{x}}_m, u, \dot{u}, \ldots, u^{(i-3)}\right) = \hat{\xi}_{e_{i+1}} + \sum_{l=1}^{m}\left\{\frac{\partial \psi_{i-1}}{\partial \hat{x}_l}\left[I_l\left[\partial \hat{H}(\bar{\hat{x}}_m)/\partial \bar{\hat{x}}_m\right]^{-1} \varepsilon^{-1} L\left[y - \hat{x}_1\right]\right]\right\}.$$

For $i = m$,

$$\dot{\hat{\xi}}_{e_m} = \dot{\psi}_{m-1}(\bar{\hat{x}}_m, u, \dot{u}, u^{(2)}, \ldots, u^{(m-3)}) = \hat{\alpha}\left(\hat{\xi}_e\right) + \hat{\beta}_1\left(\hat{\xi}_e\right)u + \ldots + \hat{\beta}_{m-1}\left(\hat{\xi}_e\right)u^{(m-2)} + \sum_{l=1}^{m}\left\{\frac{\partial \psi_{m-1}}{\partial \hat{x}_l}\left[I_l\left[\partial \hat{H}(\bar{\hat{x}}_m)/\partial \bar{\hat{x}}_m\right]^{-1} \varepsilon^{-1} L\left[y - \hat{x}_1\right]\right]\right\}.$$

$I_j \in \mathbb{R}^{1\times m}$ is a row vector whose j^{th} element is 1 and 0 otherwise. We then can write the above in matrix form as

$$\dot{\hat{\xi}}_e = A\hat{\xi}_e + B\left[\hat{\alpha}\left(\hat{\xi}_e\right) + \hat{\beta}_1\left(\hat{\xi}_e\right)u + \ldots + \hat{\beta}_{m-1}\left(\hat{\xi}_e\right)u^{(m-2)}\right] + \varepsilon^{-1} L\left[y - \hat{x}_1\right]. \tag{16}$$

Define the observer error, $\tilde{\xi}_e = \hat{\xi}_e - y_e$. Let $C \in \mathbb{R}^{1\times m} = [1, 0, \ldots, 0]$, then from (11) and (16), the observer error dynamics are given by

$$\dot{\tilde{\xi}}_e = (A - \varepsilon^{-1} LC)\tilde{\xi}_e + B\left[\hat{\alpha}\left(\hat{\xi}_e\right) + \hat{\beta}_1\left(\hat{\xi}_e\right)u + \ldots + \hat{\beta}_{m-1}\left(\hat{\xi}_e\right) u^{(m-2)}\right] - B\left[\alpha\left(y_e\right) + \beta_1\left(y_e\right)u + \ldots + \beta_{m-1}\left(y_e\right)u^{(m-2)}\right].$$

Define another coordinate transformation:

$$\tilde{v} = \varepsilon' \tilde{\xi}_e,\ \ \varepsilon' \triangleq diag\left[\frac{1}{\eta^{m-1}}, \frac{1}{\eta^{m-2}}, \ldots, 1\right].$$

In the new coordinates, the error dynamics become

$$\dot{\tilde{v}} = \frac{1}{\eta}(A - LC)\tilde{v} + B\left[\hat{\alpha}\left(\hat{\xi}_e\right) + \hat{\beta}_1\left(\hat{\xi}_e\right)u + \ldots + \hat{\beta}_{m-1}\left(\hat{\xi}_e\right) u^{(m-2)}\right] - B\left[\alpha\left(y_e\right) + \beta_1\left(y_e\right)u + \ldots + \beta_{m-1}\left(y_e\right)u^{(m-2)}\right].$$

By proper choice of L, $A - LC$ is Hurwitz. Let P be the solution to the Lyapunov equation

$$P(A - LC) + (A - LC)^T P = -I$$

and consider the Lyapunov candidate $V = \tilde{v}^T P \tilde{v} > 0$. Its time derivative along the $\tilde{v}$ trajectories is

$$\dot{V} = -\tilde{v}^T\tilde{v}/\eta + 2\tilde{v}^T PB\Big[\hat{\alpha}\left(\hat{\xi}_e\right) + \hat{\beta}_1\left(\hat{\xi}_e\right)u + \ldots + \hat{\beta}_{m-1}\left(\hat{\xi}_e\right) u^{(m-2)}\Big] - 2\tilde{v}^T PB\Big[\alpha\left(y_e\right) + \beta_1\left(y_e\right)u + \ldots + \beta_{m-1}\left(y_e\right)u^{(m-2)}\Big].$$

From Assumption 2 and the fact that $\hat{f}_i, \hat{g}_i$ are continuous differentiable functions with respect to their arguments, we have

$$\left|\hat{\alpha}\left(\hat{\xi}_e\right) - \alpha\left(\hat{\xi}_e\right)\right| \le k_1, \left|\hat{\beta}_i\left(\hat{\xi}_e\right) - \beta_i\left(\hat{\xi}_e\right)\right| \le k_{2,i},\ i = 1,\ldots,m-1,$$

where $k_1, k_{2,i}$ are bounded constants. Since $\alpha(\bullet), \beta_i(\bullet)$ and their first-order derivatives are continuous and uniformly bounded on $[t_0, t]\times\mathbb{R}^m$, from Lemma 3.3 in [15], $\alpha(\bullet), \beta_i(\bullet)$ are globally Lipschitz. Together with Assumption 3, we then have

$$\begin{aligned}
&\left|\begin{matrix}\hat{\alpha}\left(\hat{\xi}_e\right) + \hat{\beta}_1\left(\hat{\xi}_e\right)u + \ldots + \hat{\beta}_{m-1}\left(\hat{\xi}_e\right)u^{(m-2)} - \alpha\left(y_e\right) \\ -\beta_1\left(y_e\right)u - \ldots - \beta_{m-1}\left(y_e\right)u^{(m-2)}\end{matrix}\right| \\
&\quad \le k_1 + \left|\alpha\left(\hat{\xi}_e\right) - \alpha\left(y_e\right)\right| + k_{2,1}|u| + \left|\beta_1\left(\hat{\xi}_e\right) - \beta_1\left(y_e\right)\right||u| \\
&\qquad + \ldots + k_{2,m-1}\left|u^{(m-2)}\right| + \left|\beta_{m-1}\left(\hat{\xi}_e\right) - \beta_{m-1}\left(y_e\right)\right|\left|u^{(m-2)}\right| \\
&\quad \le k_3 + k_4\left|\tilde{\xi}_e\right|,
\end{aligned}$$

where k_3, k_4 are non-negative constants. Thus we have

$$\dot{V} \le -\|\tilde{v}\|^2/\eta + 2k_3\|P\|\|\tilde{v}\| + 2k_4\|P\|\|\tilde{v}\|^2.$$

We want to use part of $-\|\tilde{v}\|^2/\eta$ to dominate $2k_3\|P\|\|\tilde{v}\|$ for large $\|\tilde{v}\|$. We proceed by rewrite the foregoing inequality as

$$\dot{V} \le -(1-\theta)\|\tilde{v}\|^2/\eta + 2k_4\|P\|\|\tilde{v}\|^2, \quad \forall\|\tilde{v}\| \ge 2k_3\|P\|\eta/\theta,$$

where $0 < \theta < 1$. We can then choose $\eta < \bar{\eta}$ where $\bar{\eta} = \min\{(1-\theta)/2k_4\|P\|, 1\}$ to make

$$\dot{V} \le -W(\tilde{v}) = -\left\{(1-\theta)\|\tilde{v}\|^2/\eta - 2k_4\|P\|\|\tilde{v}\|^2\right\},$$

where $W(\tilde{v})$ is positive definite function. We then can apply Theorem 4.18 in [15] to conclude that $\tilde{v}$ and hence $\tilde{\xi}_e$ are globally uniformly ultimately bounded (GUUB). $[QED]$

APPENDIX B: PROOF OF PROPOSITION 2

We proceed by following steps.

Step 1:

The $\dot{z}_1$ equation becomes

$$\begin{aligned}
\dot{z}_1 &= f_1 + g_1x_2 + \dot{\tilde{x}}_1 - \dot{x}_{1d} + \hat{g}_1x_{2d} - \hat{g}_1x_{2d} + g_1x_{2d} - g_1x_{2d} \\
&= \left(f_1 - \hat{f}_1\right) - c_1z_1 - \hat{K}_1^T\overline{\varphi}_1 + \left(g_1 - \hat{g}_1\right)x_{2d} + g_1\left(z_2 - \tilde{x}_2\right) + \dot{\tilde{x}}_1.
\end{aligned}$$

Choose the Lyapunov function as

$$V_1 = \frac{1}{2}z_1^2 + \frac{1}{2}\tilde{K}_1^T\Gamma_{k1}^{-1}\tilde{K}_1.$$

We can find $\dot{V}_1$ as follows:

$$\begin{aligned}
\dot{V}_1 &= z_1\dot{z}_1 + \tilde{K}_1^T\Gamma_{k1}^{-1}\dot{\tilde{K}}_1 \\
&\le K_1^{*T}\varphi_1|z_1| - c_1z_1^2 - \hat{K}_1^T\overline{\varphi}_1z_1 + z_1g_1z_2 + \tilde{K}_1^T\overline{\varphi}_1z_1 - \tilde{K}_1^T\sigma_{k1}\hat{K}_1.
\end{aligned}$$

From [16], we have the property

$$0 \le |\alpha| - \alpha\frac{2}{\pi}\arctan\left(\frac{\alpha}{\eta}\right) \le 0.2785\eta, \quad \forall\alpha\in\mathbb{R}.$$

Also use the fact that

$$2\tilde{K}^T\hat{K} = \|\tilde{K}\|^2 + \|\hat{K}\|^2 - \|K^*\|^2 \ge \|\tilde{K}\|^2 - \|K^*\|^2.$$

We then have

$$\dot{V}_1 \le -c_1z_1^2 + z_1g_{1U}z_2 - \frac{\sigma_{k1}}{2}\|\tilde{K}_1\|^2 + \chi_1,$$

where

$$\chi_1 = 0.2785\eta_1\left(\varepsilon_{f_1} + \varepsilon_{g_1} + \varepsilon_{x_2} + \varepsilon_{\dot{x}_1}\right) + \frac{\sigma_{k1}}{2}\|K_1^*\|^2.$$

The term $z_1g_{1U}z_2$ will be cancelled in the next step.

Step i: $(2 \le i \le m-1)$

By using similar derivation as in Step 1, we have $\dot{z}_i$ equation as follows:

$$\begin{aligned}
\dot{z}_i &= \left(f_i - \hat{f}_i\right) - c_iz_i - g_{(i-1)U}z_{i-1} - \hat{K}_i^T\overline{\varphi}_i + \left(g_i - \hat{g}_i\right)x_{(i+1)d} \\
&\quad + g_i\left(z_{i+1} - \tilde{x}_{i+1}\right) + \dot{\tilde{x}}_i.
\end{aligned}$$

Choose the Lyapunov function as

$$V_i = V_{i-1} + \frac{1}{2}z_i^2 + \frac{1}{2}\tilde{K}_i^T\Gamma_{ki}^{-1}\tilde{K}_i.$$

The derivative $\dot{V}_i$ can be found as in the previous step to be

$$\dot{V}_i \le \sum_{l=1}^{i}\left\{-c_lz_l^2 - \frac{\sigma_{kl}}{2}\|\tilde{K}_l\|^2 + \chi_l\right\} + z_ig_{iU}z_{i+1},$$

where

$$\chi_l = 0.2785\eta_l\left(\varepsilon_{f_l} + \varepsilon_{g_l} + \varepsilon_{x_{i+1}} + \varepsilon_{\dot{x}_l}\right) + \frac{\sigma_{kl}}{2}\|K_l^*\|^2.$$

The term $z_ig_{iU}z_{i+1}$ will be cancelled in the next step.

Step m:

This is the last step. We have

$$\begin{aligned}
\dot{z}_m &= \left(f_m - \hat{f}_m\right) - c_mz_m - g_{(m-1)U}z_{m-1} - \hat{K}_m{}^T\overline{\varphi}_m \\
&\quad + \left(g_m - \hat{g}_m\right)u + \dot{\tilde{x}}_m.
\end{aligned}$$

Choose the Lyapunov function as

$$V_m = V_{m-1} + \frac{1}{2}z_m^2 + \frac{1}{2}\tilde{K}_m^T\Gamma_{km}^{-1}\tilde{K}_m = \sum_{l=1}^{m}\left\{\frac{1}{2}z_l^2 + \frac{1}{2}\tilde{K}_l^T\Gamma_{kl}^{-1}\tilde{K}_l\right\}.$$

The derivative $\dot{V}_m$ can be found as in the previous step to be

$$\dot{V}_m \le \sum_{l=1}^{m} \left\{ -c_l z_l^2 - \frac{\sigma_{kl}}{2} \left\| \tilde{K}_l \right\|^2 + \chi_l \right\}.$$

Let $\varsigma = \min_{1 \le l \le m} \{2c_l\} > 0$, $\delta = \sum_{l=1}^{m} \chi_l \ge 0$ and choose $\sigma_{kl} \ge \varsigma \lambda_{\max} \left\{ \Gamma_{kl}^{-1} \right\}$, $l = 1, \ldots, m$,

using the Rayleigh-Ritz inequality, we have

$$\dot{V}_m \le \sum_{l=1}^{m} \left\{ -\varsigma 0.5 z_l^2 - \varsigma 0.5 \tilde{K}_l^T \Gamma_{kl}^{-1} \tilde{K}_l + \chi_l \right\} \le -\varsigma V_m + \delta.$$

We wish to find some positive definite function $W\left(\left\|\left\{z_i, \tilde{K}_i\right\}\right\|\right)$ such that $\dot{V}_m \le -W\left(\left\|\left\{z_i, \tilde{K}_i\right\}\right\|\right)$ when $\left\|\left\{z_i, \tilde{K}_i\right\}\right\| \ge \mu$, proving that the trajectory $z_i, \tilde{K}_i$ are globally uniformly ultimately bounded. From Lemma 4.3 in [15], since we have $V_m > 0$ and radially unbounded, there exist class K_∞ functions, α_1, α_2 such that $\alpha_1\left(\left\|\left\{z_i, \tilde{K}_i\right\}\right\|\right) \le V_m \le \alpha_2\left(\left\|\left\{z_i, \tilde{K}_i\right\}\right\|\right)$. Choose some θ such that $0 < \theta < 1$. Then

$$\dot{V}_m \le -\theta\varsigma V_m - (1-\theta)\varsigma V_m + \delta \le -\theta\varsigma\alpha_1 - (1-\theta)\varsigma V_m + \delta.$$

Choosing $W = \theta\varsigma\alpha_1$ we see that

$$\dot{V}_m \le -W - (1-\theta)\varsigma V_m + \delta.$$

Therefore if $\left\|\left\{z_i, \tilde{K}_i\right\}\right\| \ge \mu$ where $\mu = \alpha_1^{-1}\left(\delta/(1-\theta)\varsigma\right)$ then $(1-\theta)\varsigma V_m \ge (1-\theta)\varsigma\alpha_1(\mu) = \delta$. Thus $\dot{V}_m \le -W$ for all $\left\|\left\{z_i, \tilde{K}_i\right\}\right\| \ge \mu$. Therefore from Theorem 4.18 in [15], the trajectory $z_i, \tilde{K}_i$ are GUUB. $[QED]$

REFERENCES

[1] E. B. Kosmatopoulos, M. M. Polycarpou, M. A. Christodoulou, and P. A. Ioannou, "High-order neural network structures for identification of dynamical systems," *IEEE Trans. Neural Networks,* vol. 6, no. 2, pp. 422-431, Mar. 1995.

[2] R. M. Sanner, and J. J. E. Slotine, "Gaussian networks for direct adaptive control," *IEEE Trans. Neural Networks,* vol. 3, no. 6, pp. 837-863, Nov. 1992.

[3] I. Ciuca, and J. A. Ware, "On the (1+1/2) layer neural networks as universal approximators," in *1998 IEEE Int. Conf. Neural Networks,* pp. 1218-1223.

[4] R. K. Elsley, and M. S. Lan, "Application of neural networks to adaptive control," in *Proc. of 22nd Asilomar Conf. on Signals, Systems and Computers,* 1988, pp. 517-522.

[5] G. W. Ng, *Application of Neural Networks to Adaptive Control of Nonlinear Systems.* New York: John Wiley, 1997.

[6] G. A. Rovithakis, "Robustifying Nonlinear Systems using High Order Neural Network Controllers," *IEEE Trans. Automatic. Control.,* vol. 44, no. 1, pp. 102-108, 1999.

[7] S. Wu, M. J. Er and Y. Gao, "A fast approach for automatic generation of fuzzy rules by generalized dynamic fuzzy neural networks," *IEEE Trans. Fuzzy Systems,* vol. 9, no. 4, pp. 578-594, August 2001.

[8] J. S. R. Jang, "ANFIS: adaptive-network-based fuzzy inference system," *IEEE Trans. Systems, Man and Cybernetics,* vol. 23, no. 3, May,Jun. 1993.

[9] J. S. R. Jang, C. T. Sun, and E. Mizutani, *Neuro-Fuzzy and Soft Computing.* New Jersey: Prentice-Hall, 1997, pp. 342-344.

[10] J. T. Spooner, M. Maggiore, R. Ordonez, and K. M. Passino, *Stable Adaptive Control and Estimation for Nonlinear Systems.* New York: Wiley Interscience, 2002, ch. 10.

[11] M. Krstic, I. Kanellakopoulos, and P. Kokotovic, *Nonlinear and Adaptive Control Design.* New York: Wiley Interscience, 1995.

[12] S. S. Ge, C. C. Hang, T. H. Lee and T. Zhang, *Stable Adaptive Neural Network Control*. The Netherlands: Kluwer Academic Publishers, 2002, ch. 4.

[13] R. A. DeCarlo, S. H. Zak, and G. P. Matthews, "Variable structure control of nonlinear multivariable systems," in *Proc. of the IEEE*, vol. 76, no. 3, Mar. 1988, pp. 212-232.

[14] K. J. Astrom, and B. Wittenmark, *Adaptive Control.* Addison-Wesley, 1995, ch. 11.

[15] H. K. Khalil, *Nonlinear Systems.* Englewood Cliffs, NJ: Prentice Hall, 2002.

[16] M. M. Polycarpou and P. A. Ioannou, "A robust adaptive nonlinear control design," *Automatica,* vol. 32, pp. 423-427, 1996

[17] W. Chatlatanagulchai, H. C. Nho and P. H. Meckl, "Robust observer backstepping neural networks control of flexible-joint manipulator," in *Proc. American Control Conference,* Boston, 2004, pp. 3035-3040.

		Value in SI units
θ_m	Absolute motor angular position	
θ_s	Absolute sprocket angular position	
θ_l	Absolute link angular position	
a	Distance from sprocket center to link C.G.	0.09443 m
b	Distance from sprocket center to payload C.G.	0.254 m
J_m	Motor inertia about motor C.G.	0.000525 $kg \cdot m^2$
J_s	Sprocket inertia about sprocket C.G.	0.00005 $kg \cdot m^2$
J_l	Link inertia about link C.G.	0.07 $kg \cdot m^2$
J_p	Payload inertia about payload C.G.	0.0005 $kg \cdot m^2$
m_l	Link mass	3.545 kg
m_p	Payload mass	1.0 kg
k	Spring stiffness coefficient	6.77 N/m
d	Spring internal damping	0.001507 $N \cdot s/m$
c_m	Coefficient of viscous friction at motor bearing	0.02
c_l	Coefficient of viscous friction at joint bearing	0.01
r	Gear ratio	5.3

Table 1. Description of parameters and their values used in the simulation.

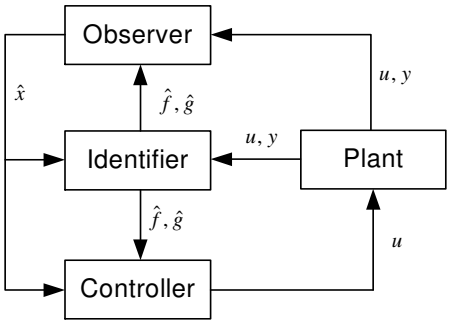

Fig. 1. Observer-identifier-controller system diagram.

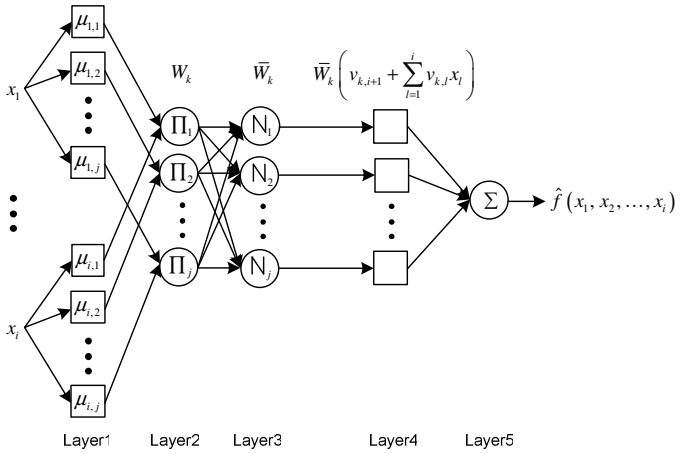

Fig. 2. Adaptive Neuro-Fuzzy Inference Systems (ANFIS).

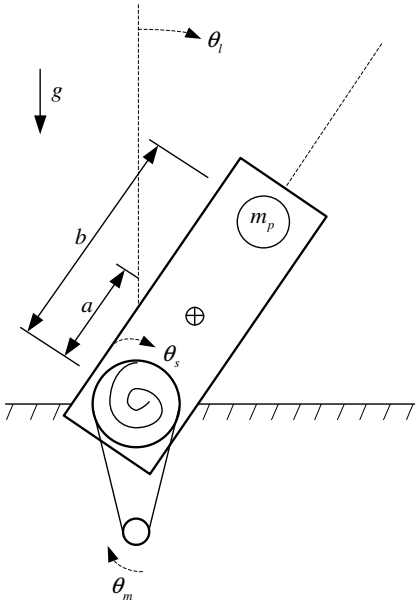

Fig. 3. Schematic diagram of one-link flexible-joint robot manipulator.

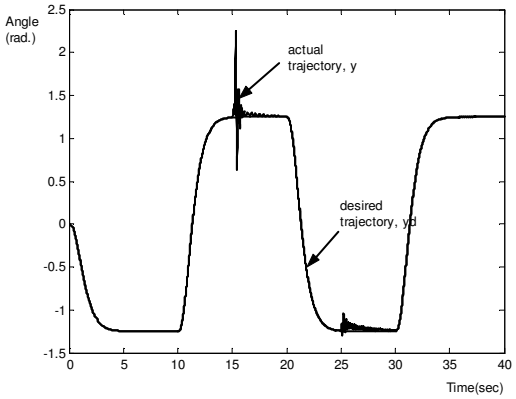

Fig. 4. Tracking performance under payload variation. Payload is changed from m_p = 1 kg to m_p = 4 kg at 15 sec and back to 1 kg at 25 sec.

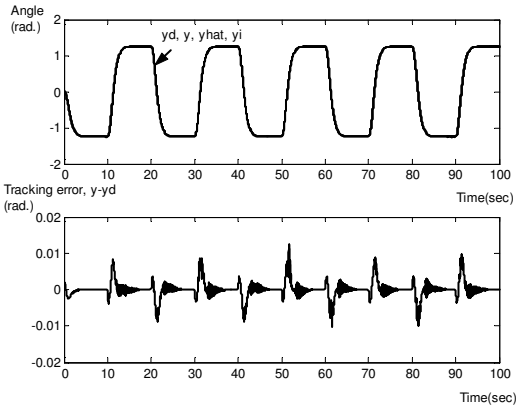

Fig. 5. Tracking performance over 100 sec. (Top) Comparison among actual output y, desired output y_d, estimated state $\hat{y} = \hat{x}_1$ and identifier state $y_i = \xi_1$. (Bottom) Tracking error $y - y_d$.

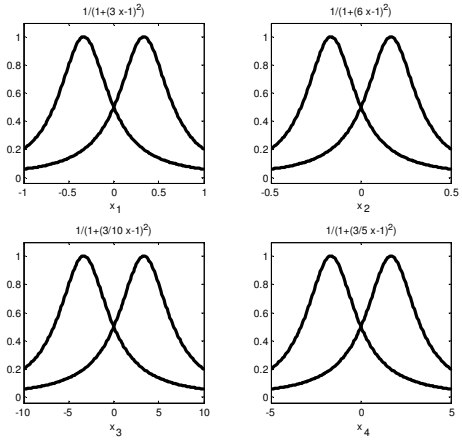

Fig. 6. Membership functions in layer 1 of ANFIS.

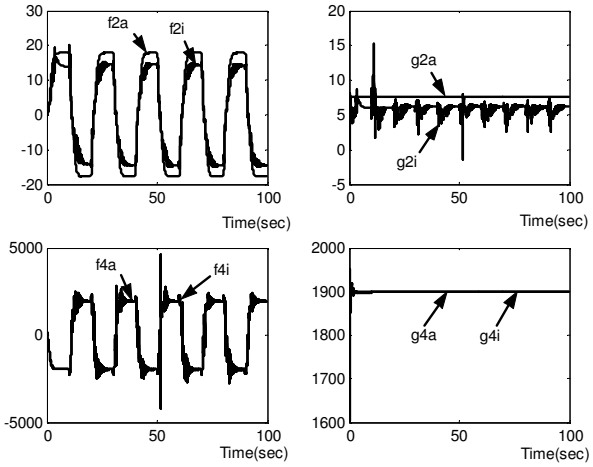

Fig. 7. Comparison between actual plant functions and identified plant functions.

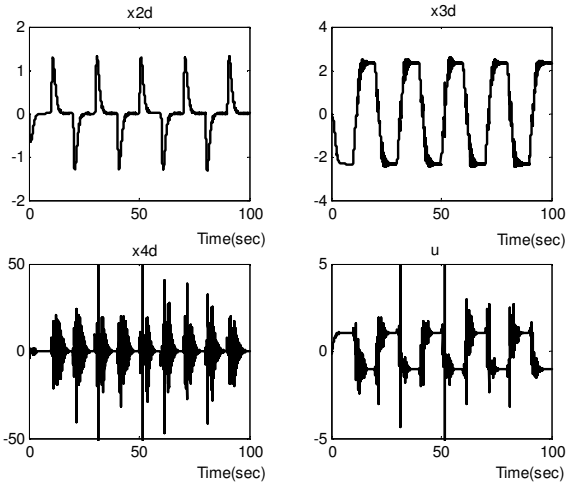

Fig. 8. Virtual control inputs x_{2d}, x_{3d}, x_{4d} and actual control input u.